International Journal of Rail Transportation

ISSN: (Print) (Online) Journal homepage: https://www.tandfonline.com/loi/tjrt20

Multi-objective optimization of high-speed train suspension parameters for improving hunting stability

Xiangwang Chen, Yuan Yao, Longjiang Shen & Xiaoxia Zhang

INTERNATIONAL JOURNAL OF RAIL TRANSPORTATION
https://doi.org/10.1080/23248378.2021.1904444

Multi-objective optimization of high-speed train suspension parameters for improving hunting stability

Xiangwang Chen[a], Yuan Yao[a], Longjiang Shen[b] and Xiaoxia Zhang[a,c]

[a]State Key Laboratory of Traction Power, Southwest JiaoTong University, Chengdu, People's Republic of China; [b]Technology Centre, CRRC Zhuzhou Locomotive Co., Ltd, Zhuzhou, People's Republic of China; [c]College of Nuclear Technology and Automation Engineering, Chengdu University of Technology, Chengdu, People's Republic of China

ABSTRACT

Excellent hunting stability is required for the operation of high-speed trains. The suspension parameter design needs to avoid primary and secondary hunting instability for the low and high wheel–rail contact conicity, respectively, as well as to enhance the robustness of hunting stability in face of the variations in wheel–rail contact parameters. In this paper, the indices of low equivalent conicity stability, high conicity stability, and equivalent conicity robustness are defined and chosen as the optimization objectives for the optimal design of key suspension parameters. The multi-objective optimization method is used, and the obtained Pareto set can guide the matching laws of suspension parameters. Four groups of typical parameter sets are selected, and their stability characteristics, such as speed robustness and equivalent conicity robustness, are analysed in detail, followed by the selection of equivalent conicity and motor flexible suspension parameters. Two parameter design modes for the hunting stability can be reflected.

ARTICLE HISTORY
Received 8 October 2020
Revised 13 March 2021
Accepted 13 March 2021

KEYWORDS
High-speed train; suspension parameter design; hunting stability; multi-objective optimization; motor flexible suspension

1. Introduction

With the increasing operation speed of high-speed trains, more attention should be paid to the hunting stability of the vehicle system [1], which is closely related to the ride comfort and running safety against the derailment of train operation. At present, several methods have been put forward to improve the running stability of vehicles, of which active suspension technology is typical and has a good effect [2–6]. However, widespread adoption of it into service operation has not taken place for several problems in practical applications, such as numerous components, inconvenient maintenance, high costs, etc. [7]. Thus, the optimization of traditional passive suspension still can be considered as a basic method to improve the lateral running stability of vehicles [8–11]. Even though analysing the influence laws of suspension parameters on vehicle performances can guide the optimal design, it's difficult to comprehensively consider the combined effects of multiple suspension parameters on vehicle hunting stability if the suspension parameter combination is limited and analysis cases are few.

CONTACT Yuan Yao yyuan8848@163.com State Key Laboratory of Traction Power, Southwest Jiaotong University NO.111, North Section 1, Second Ring Road Chengdu, Sichuan, 610031 P.R. China

The optimal design of mechanical systems aims at finding a trade-off scheme in consideration of complex and contradictory indices to meet good comprehensive performance requirements [12–14]. Determining suspension parameters of railway vehicles is a typical multi-objective optimization problem, in which the selection of suspension parameters needs to weigh multiple performance indices. Focusing on the problems of running safety, ride comfort and wheel profile wear of a railway vehicle, Johnsson et al. [15] carried out the multi-objective optimal design on damping elements and adopted an adaptive control strategy to further improve vehicle performances. Bideleh et al. [16] established a 50-degree-of-freedom simulation model of the railway vehicle, which considered the arrangement symmetries of primary and secondary suspensions. Various operating scenarios of straight lines and curves were analysed, and the optimization problem of wheel–rail wear and ride comfort of vehicles was solved by using the genetic algorithm. The robustness of bogie dynamic responses to suspension parameter uncertainties was also further explored [17]. Jiang Y et al. [18] built a train model consisting of six car bodies and seven straddle-type bogies for a certain articulated monorail vehicle operating in China. The curve passing performance of the train was improved by virtue of the genetic algorithm, and ride quality, comfort and wear indices were significantly ameliorated by adopting optimized suspension parameters. Yao Y et al. [19] put forward the concept of robustness of hunting stability, which was chosen as the optimization objective for suspension parameters optimum of the high-speed train bogie. Special attention was put on the distribution of optimized suspension parameters to obtain the matching rules for key suspension parameters, and the multivariate statistical analysis was carried out to explore the correlation between suspension parameters and each stability index. At present, researches on suspension parameter optimization of railway vehicles mainly focus on the compromise design of running performance on tangent track, curve negotiation performance and wheel–rail wear performance.

This paper concentrates on the hunting stability of high-speed trains, and the general idea for suspension parameter design is illustrated. The bogie suspension parameters are reasonably selected to obtain an adequate stability margin of the train operating in distinct wheel–rail contact states and to enhance the ability to resist the influence caused by the change in wheel–rail contact parameters on hunting stability, which means that the train will have good adaptability to tracks. Based on the above factors, the design of suspension parameters which remarkably affect the hunting stability of the vehicle is a typical multi-objective and multi-parameter optimization problem. The optimization objectives for vehicle hunting stability are defined in this paper, and several key suspension parameters affecting vehicle performances are simultaneously optimized to get optimal suspension parameter sets, whose corresponding characteristics of vehicle hunting stability are analysed in detail. Then, the matching suspension parameters of the motor suspended flexibly under the bogie frame are optimized and selected. This multi-objective optimization method is able to provide the reference for the design of train suspension parameters, achieving different performance requirements.

2. Lateral dynamics model of the vehicle

As shown in Figure 1, a simplified lateral dynamics model of a typical Chinese high-speed train is established [19]. The specific parameters of the model are shown in Appendix Table A1. The model is composed of seven rigid bodies. The wheelset and the frame have

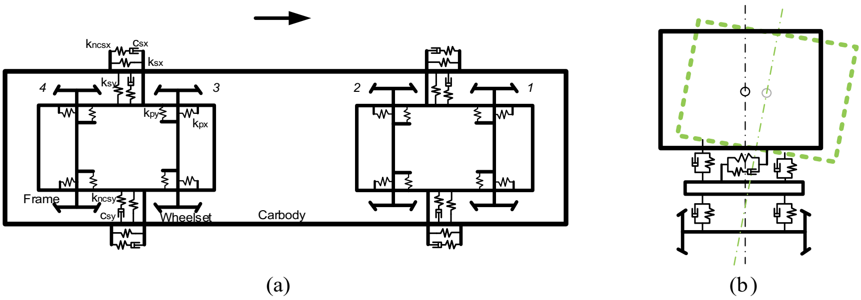

Figure 1. Simplified vehicle lateral dynamics model.

lateral and yaw degrees of freedom, and the car body has lateral, yaw and roll degrees of freedom. The wheelset is connected with the frame through the primary suspension, which is comprised of lateral, longitudinal and vertical positioning stiffness. Besides, the primary rotating arm axle box structure is considered. Secondary lateral, longitudinal and vertical stiffness and damping are placed between the frame and the car body, and the anti-roll stiffness is also taken into account. In order to analyse the influence of stiffness effect and damping effect on vehicle stability, the oil damper is simulated based on the Maxwell model that consists of damping and stiffness in series [20]. A hypothetical mass block of infinitesimal quality exists between the damping and stiffness to facilitate the establishment of the dynamic equations for the vehicle system. As a result, the dynamics model has a total of 27 degrees of freedom considering additional degrees of freedom introduced by the damper model. The linear stability of the vehicle system is investigated in this paper; hence, it is assumed that the suspension characteristics of the primary and secondary suspensions are linear. The wheel–rail contact geometry is expressed by the equivalent conicity, and the wheel–rail creep force is calculated by linear Kalker theory as it is considered to work in the linearity range. The equation of the system dynamics model can be written as

$$\mathbf{M}\ddot{\mathbf{x}} + \mathbf{C}\dot{\mathbf{x}} + \mathbf{K}\mathbf{x} = \mathbf{Q} \tag{1}$$

where $\mathbf{x}$ is the degree of freedom vector of the system. **M, C, K,** and **Q** are the mass, damping, stiffness, and external force matrices of the system, respectively. The matrix **K** is an asymmetric matrix, including items of the suspension stiffness, gravitational stiffness, and creep stiffness. The creep stiffness does positive work and injects energy into the system, which is the source of hunting instability. However, the suspension and creep damping of the matrix **C** both do negative work to dissipate system energy [21]. In a period of hunting motion, the vehicle system will be in a critical stable state if the input and consumed energy are equal. Since the linear stability of the vehicle system is emphatically analysed, the matrix **Q** is set to a null vector. The complex modal transformation is adopted to obtain the state space equation,

$$\ddot{\mathbf{y}}(t) = \mathbf{A}\mathbf{y}(t) \tag{2}$$

where the system state vector $\mathbf{y}(t)=[\mathbf{x}(t), \dot{\mathbf{x}}(t)]^{\mathrm{T}}$, and the system matrix **A** is given by

$$\mathbf{A} = \begin{bmatrix} \mathbf{0}_{27\times27} & \mathbf{I}_{27\times27} \\ -\mathbf{M}^{-1}\mathbf{K} & -\mathbf{M}^{-1}\mathbf{C} \end{bmatrix} \tag{3}$$

By solving the eigenvalues and eigenvectors of the matrix **A**, the linear stability indices and the corresponding modal shapes of the vehicle system can be obtained.

3. Multi-objective optimization of suspension parameters

3.1. Multi-objective optimization problem

Objective functions often conflict with each other in multi-objective optimization, and the improvement of one objective performance may lead to the deteriorations of other objective performances; thus, it is difficult to find an ideal solution to make all optimization objectives optimal at the same time. Some classical methods try to scalarize the objective vector into one objective [22,23], such as methods of objective weighting, distance functions, and min-max formulation. However, these algorithms are sensitive towards weights or demand levels and require knowledge of the individual optimum prior to vector optimization, which result in the difficulty in applying these classical methods to engineering practice directly. Furthermore, multiple alternative solutions, instead of the unique optimal solution obtained in single-objective optimization, may be desired because decision makers are able to choose one appropriate solution from them according to changing situations.

The following Pareto optimal concepts are usually involved in the multi-objective optimization problem [24].

(a) In the problem of minimizing objective functions, let $\mathbf{u} = [u_1, u_2, \ldots, u_n]^T$ and $\mathbf{v} = [v_1, v_2, \ldots, v_n]^T$ are two target vectors in decision space, if $f_i(\mathbf{u}) \leq f_i(\mathbf{v})$ and $\mathbf{u} \neq \mathbf{v}$ for all objective functions, then the vector **v** is called dominated by the vector **u**.
(b) The vector is called a Pareto optimal if there is no vector which dominates it in decision space.
(c) The set of all Pareto optimal solutions is called the Pareto set ($\mathbf{P}_s$).
(d) The image of Pareto set in objective function space is called the Pareto front ($\mathbf{P}_f$), which is denoted as

$$\mathbf{P}_f = \{\mathbf{F}(\mathbf{x}) \in \mathbf{R}^m | \mathbf{x} \in \mathbf{P}_s\} \tag{4}$$

Two goals in multi-objective optimization should be achieved. That is, the obtained solutions are desired to converge to the true Pareto set as closely as possible, and they ought to be distributed uniformly in the entire Pareto optimal region.

3.2. NSGA-II

There are numerous effective algorithms to solve multi-objective optimization problems, a fast non-dominated sorting genetic algorithm NSGA-II with the elitist strategy is chosen in this study [25]. NSGA-II is developed from NSGA, some drawbacks of NSGA can be overcome, such as high computational complexity of nondominated sorting, lack of elitism, and need for specifying the sharing parameter. Three innovations, including the fast non-dominated sorting, crowded distance estimation, and simple crowded comparison operator, are introduced to get the more accurate Pareto front and to reduce operational complexity. Population diversity and computational efficiency can be improved remarkably.

The algorithm comprises the following procedures [22,25]. It starts with the initialization of a random parent population P_0 that satisfies the constraints on decision variables. Then, the non-dominated sorting is carried out, in which the population is sorted based on non-domination and each solution is assigned a non-domination rank. To achieve diversity preservation, a parameter called the crowding distance is defined and calculated, its large value indicates a great diversity of the solution. In the next stage, the binary tournament selection is performed to get the parent population P_{0s} for the next generation, the selection of solutions is based on the non-domination rank and crowding distance. Then, recombination and mutation operators are applied to create an offspring population Q_0 of size N, which merges with P_{0s} to form a combined population R_0. This guarantees the elitism of the best individuals. In the last stage, the population R_0 is sorted based on non-domination, the members of new population P_1 are chosen from each front subsequently until the population size exceeds N. For the last front selected, if its all members cannot be accommodated, then the individuals are selected according to their crowding distances in the descending order until all population slots are filled. The process is repeated until the maximum generation is reached.

3.3. Multi-objective optimal design

The hunting stability and curve passing performance of the vehicle are usually contradictory. Considering the curve radius of the track on which high-speed passenger trains run are larger, the curve negotiation problem is downgraded to a secondary status, and ensuring the lateral running stability of the vehicle should be given priority in the optimal design of suspension parameters. During the vehicle operation, wheel–rail profile wear and the track deformation will change the wheel–rail contact relationship and lead to the change of wheel–rail matching conicity, which has a significant impact on hunting stability. When the wheel–rail contact conicity is lower, especially in the situation of a larger rail cant, the newly re-profiled wheel tread and the newly grinded rail, since a lower hunting frequency is close to the suspension frequency of the car body, primary hunting instability is prone to occur. The low-frequency lateral oscillation of the car body arises, seriously affecting the ride comfort and even running safety of the vehicle. At the late wheel reprofiling interval, however, wheel profile wear could lead to an increase in the wheel–rail contact equivalent conicity, in which case the insufficient vehicle stability margin will induce secondary hunting instability, manifesting as the lateral violent vibration of the bogie. Additionally, the coupling of higher hunting frequency and car body's structural frequency may happen, generating the high-frequency vibration of the car body. Therefore, special attention should be paid to the hunting stability of the vehicle with lower or higher equivalent conicity. With an appropriate stability margin, the vehicle will not experience hunting instability and the wheel tread as well as rail head will be worn uniformly. Furthermore, high-speed trains require the strong ability to resist the influence of wheel–rail contact parameter perturbations on lateral stability, so as to prevent an abrupt change to vehicle stability caused by variations in line conditions. Such an ability is called equivalent conicity robustness, which reflects the adaptability of trains to the track variation.

The eigenvalues of the system matrix **A** are calculated for the aforesaid linear vehicle dynamics model. The ratio of the real part of eigenvalue to the modulus corresponding to hunting modal is defined as the linear stability index ζ [4], which is the opposite number of the natural modal damping ratio. Generally, the positive value of the damping ratio indicates that the system is stable. Therefore, the negative value of ζ corresponds to the stable state of the vehicle system. This facilitates the following multi-objective optimization design, in which a smaller value of the optimization objective is regarded as a better one. ζ_{low} and ζ_{high} are two stability indices corresponding to the low equivalent conicity and high equivalent conicity, respectively. The smaller the index value is, the more stable the vehicle system is. In order to evaluate the adaptability of high-speed trains to different line conditions, the standard deviation of the stability indices with the equivalent conicity distributed in a certain range is calculated and defined as the equivalent conicity robustness index $std(\zeta_\lambda)$. The smaller its value is, the slighter the influence of the equivalent conicity perturbation on the hunting stability of the vehicle system is, and the stronger the adaptability to track variations is. The running condition settings of the three optimization objectives are shown in Table 1.

Four suspension parameters that significantly affect the hunting stability of the vehicle, including the primary longitudinal stiffness *Kpx*, the primary lateral stiffness *Kpy*, the damping of yaw damper *Csx* and the yaw damper series stiffness *Kncsx*, are optimized to minimize the objective functions. The multi-objective optimization problem can be stated as

$$\min\{\zeta_{low}, \zeta_{high}, std(\zeta_\lambda)\} \tag{5}$$

The NSGA-II algorithm is used for this multi-objective and multi-parameter optimization problem. Most of the default settings of the algorithm keep invariant, and only the population size and generation number are changed, which are set to 3000 and 30 respectively in this study for the consideration of population diversity and computational burden.

3.4. Multi-objective optimization results

The secondary lateral damping *Csy* can effectively inhibit hunting motion, playing an important role in ensuring the lateral stability of the vehicle. Referring to the damping values adopted by Chinese high-speed trains, secondary lateral damping is set to 10, 25, and 40 kN.s/m, respectively. The Pareto fronts, as shown in Figure 2, are achieved by iteration and updating suspension parameters to optimize the vehicle system

Table 1. Stability indices and their calculation conditions.

	Calculation condition	
	V (km/h)	λ
ζ_{low}	200	0.05
ζ_{high}	350	0.4
$std(\zeta_\lambda)$	350	0.05 ~ 0.3

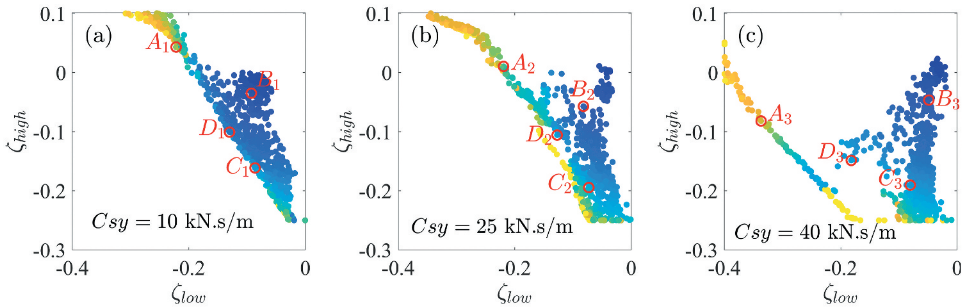

Figure 2. Pareto fronts of the multi-objective optimization.

performances towards the defined objectives. In the figure, the abscissa axis and the vertical axis represent the low equivalent conicity stability index ζ_{low} and the high equivalent conicity stability index ζ_{high}, respectively. The smaller the index value is, the better the stability of the corresponding hunting motion is. The colour of the data point indicates the equivalent conicity robustness index $std(\zeta_{\lambda})$, and the darker the colour is, the better equivalent conicity robustness is, which means that the vehicle has strong track adaptability and a long wheel tread reprofiling interval.

The Pareto fronts corresponding to different *Csy* are distinct. The one corresponding to a larger *Csy* is distributed more discretely and better low equivalent conicity stability can be achieved there. The Pareto fronts illustrate the contradiction among optimization objectives. High equivalent conicity stability tends to decline as low conicity stability continues to improve, especially under the condition of a smaller *Csy*. And equivalent conicity robustness can be improved at the expense of the system stability. The optimal suspension parameters corresponding to desired objective functions can be artificially selected according to different design requirements. What needs to be noticed is that in the optimal design of suspension parameters, which cannot be considered as complete mathematical optimization, actual project conditions should be taken into account.

Exploring the distribution characteristics of the optimal suspension parameters, the Pareto sets are obtained for this multi-objective optimal design, as depicted in Figure 3. The horizontal axis represents the low conicity stability index, and the vertical axis represents the optimal suspension parameter. The colour of the data point indicates the normal equivalent conicity stability index ζ_{norm}, which is a reflection of the vehicle stability under the condition that the running speed is 350 km/h and the wheel–rail contact equivalent conicity is 0.15. The darker the colour is, the better the vehicle system stability is.

When the secondary lateral damping *Csy* is 10 kN.s/m, the optimal solutions of *Csx* are less than those of the other two cases, mostly not more than 1000 kN.s/m. When *Csy* is selected as 40 kN.s/m, the optimal solutions of *Kpy* are small and concentrated, and they are located at the range of 3–8 kN/mm. However, the optimal solution distribution of *Csx* is polarized, with the damping being either a larger value of more than 3000 kN.s/m or a smaller value of less than 1000 kN.s/m. And low equivalent conicity stability and normal conicity stability are more outstanding when *Csy* is selected as a larger value. When *Csy* is set to 25 kN.s/m, the distribution of the optimal solutions for each suspension parameter is more dispersed and the parameter matching is more diversified.

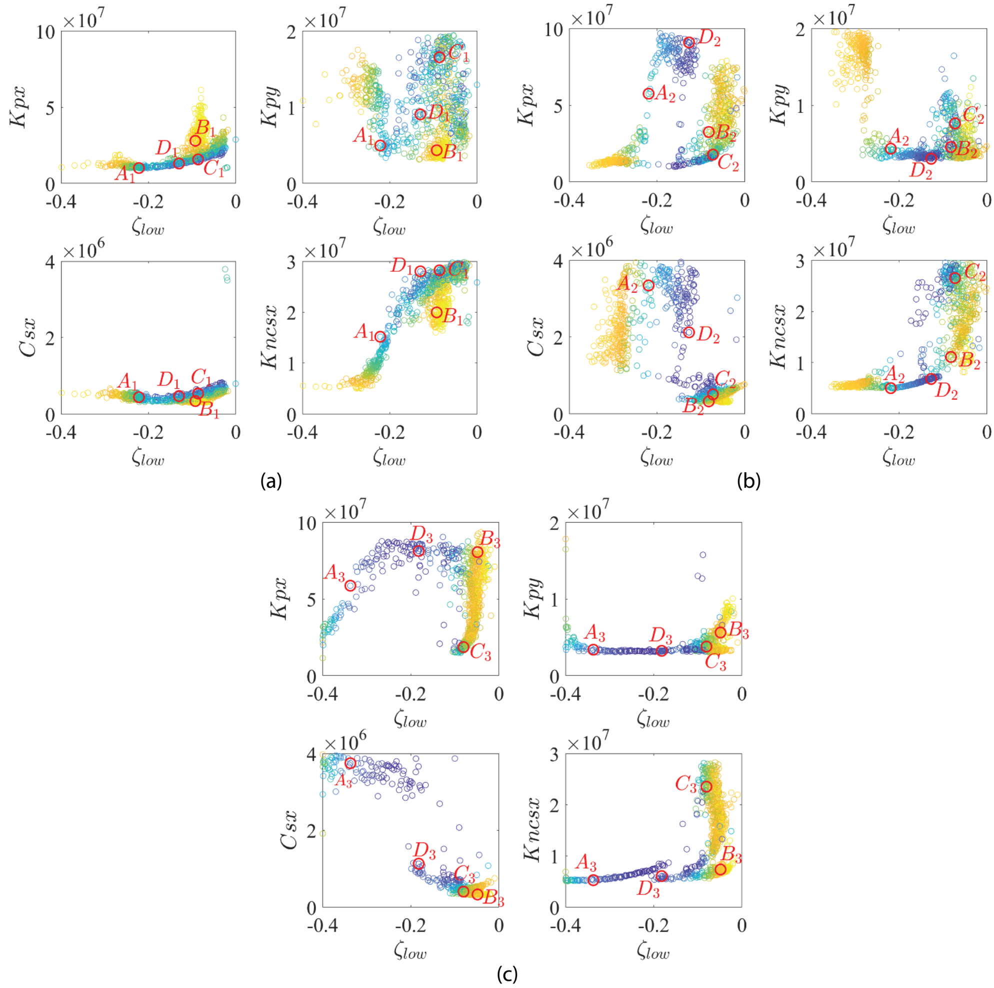

Figure 3. Pareto sets of the multi-objective optimization. (a) *Csy*=10 kN.s/m; (b) *Csy*=25 kN.s/m; (c) *Csy*=40 kN.s/m.

More significantly, for the three kinds of values of *Csy, Kncsx* has the same influence on the stability of the vehicle with the low equivalent conicity, that is, ζ_{low} decreases with the decreasing value of *Kncsx*, hence reducing the value of *Kncsx* is conducive to improving the hunting stability of the vehicle with the low equivalent conicity. In addition, the selection of a larger *Csy* is in favour of the integration of good normal equivalent conicity stability and low equivalent conicity stability, namely the coexistence of the small ζ_{norm} and small ζ_{low}.

4. Analysis of stability robustness

Four groups of representative optimal solutions of the suspension parameters are extracted from each Pareto set and indicated as *Par A, Par B, Par C,* and *Par D* respectively for further analysis, whose specific values are shown in Table 2.

Table 2. Typical optimal suspension parameters and corresponding objective performance indices.

Csy (kN.s/m)	*Kpx* (kN/mm)	*Kpy* (kN/mm)	*Csx* (kN.s/m)	*Kncsx* (kN/mm)	ζ_{low}	ζ_{high}	$std(\zeta_\lambda)$	*Par*
10	10.2	5.00	443.4	15.2	−0.22	0.04	0.14	A_1
10	28.1	4.38	340.2	20	−0.09	−0.03	0.02	B_1
10	15.9	16.6	537.6	28.2	−0.09	−0.16	0.07	C_1
10	13.2	9.08	471.3	28	−0.13	−0.10	0.06	D_1
25	57.6	4.35	3343	5.03	−0.22	0.01	0.11	A_2
25	32.7	4.57	326	11.1	−0.08	−0.06	0.03	B_2
25	17.9	7.64	507.9	26.5	−0.07	−0.19	0.08	C_2
25	91.0	3.03	2120	6.82	−0.13	−0.11	0.08	D_2
40	58.8	3.41	3750	5.27	−0.34	−0.08	0.12	A_3
40	80.7	5.65	331.2	7.35	−0.05	−0.05	0.03	B_3
40	18.7	3.82	405.4	23.5	−0.08	−0.19	0.07	C_3
40	81.4	3.26	1130	6.07	−0.18	−0.15	0.07	D_3

According to the values of *Csx*, the suspension parameter sets in the table can be divided into two types. The first one is a combination of the large *Csx* and small *Kncsx*, while the second one includes the small *Csx*, and the matching *Kncsx* is mostly larger. The performance indices and optimal parameter values corresponding to each suspension parameter set are marked in Figures 2 and 3. *Par A, Par B,* and *Par C* correspond to excellent low equivalent conicity stability, equivalent conicity robustness, and high equivalent conicity stability, respectively, and *Par D* gives consideration to all three objective performances, achieving the most comprehensive stability of the vehicle system. Even though the vehicle objective performances obtained by adopting different optimal suspension parameter sets vary, they can improve the hunting stability of the vehicle from different perspectives, thus ensuring the running safety and ride comfort of high-speed trains.

The variations of vehicle system stability with the change of equivalent conicity are analysed at different speed levels, as shown in Figure 4. The horizontal axis of each

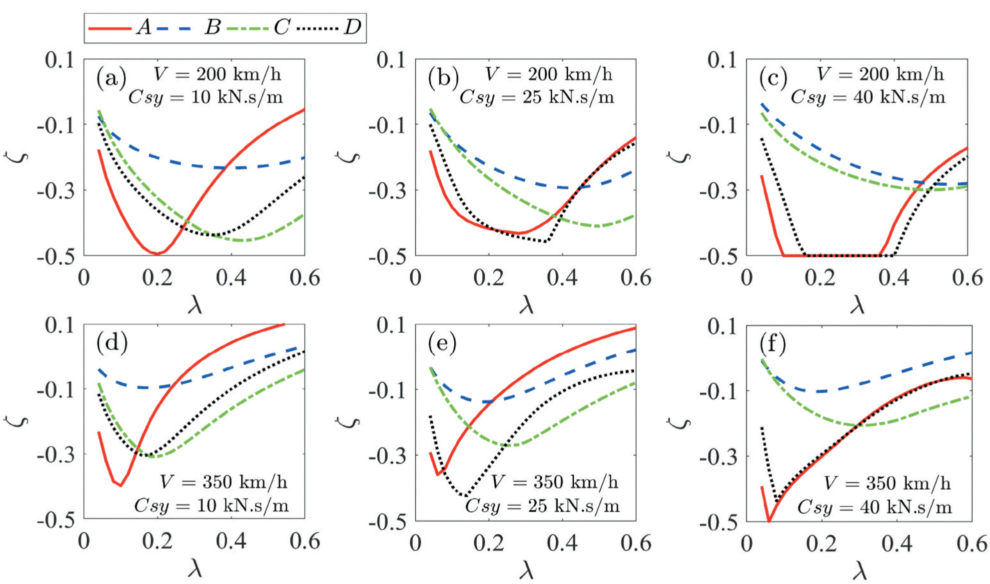

Figure 4. Linear stability varying with equivalent conicity.

subgraph represents the equivalent conicity varying from 0.04 to 0.6, and the vertical axis represents the linear stability index ζ. When the vehicle speed is 200 or 350 km/h, there is an optimal matching equivalent conicity for each suspension parameter set, and the optimal equivalent conicity corresponding to the speed of 350 km/h is lower. When *Csy* is 10 kN.s/m, hunting instability can occur for the vehicle equipped with the suspension parameters of $Par\ A_1$ in the situation of high equivalent conicity. The vehicle system stability corresponding to $Par\ B_1$ is insensitive to the change of wheel–rail contact equivalent conicity, which indicates that the vehicle has strong adaptability to tracks, but has the potential for insufficient stability margin. And the suspension parameters of $Par\ C_1$ and $Par\ D_1$ can match a wide range of equivalent conicity to obtain good lateral stability of the vehicle. When *Csy* is set to 25 or 40 kN.s/m, the stability indices corresponding to *Par B* and *Par C* show the similar variation tendency and have strong equivalent conicity robustness, especially for *Par B*. A large stability margin can be obtained by matching the suspension parameters of *Par A* and *Par D* with the reasonable equivalent conicity, but the hunting stability is sensitive to the variation of equivalent conicity.

Comparing the objective performances of the four types of suspension parameter sets, and then the parameter set corresponding to the relatively outstanding vehicle performances is selected from each type, as shown in Table 3. These selected suspension parameter sets can be divided into two types. Among them, suspension parameters of *Par A* and *Par D* include a larger *Csx* and a smaller *Kncsx*, with which the vehicle system with the low equivalent conicity has good hunting stability. However, the vehicle system equipped with suspension parameters of *Par B* and *Par C*, which include a smaller *Csx* and a larger *Kncsx*, has excellent equivalent conicity robustness. In order to analyse the speed robustness to lateral stability of the vehicle system equipped with the four groups of selected suspension parameter sets, the root loci of the vehicle system with the change of running speed are shown in Figure 5. Each root locus is composed of 40 sets of characteristic roots in the speed range of 20–800 km/h. The wheel–rail contact equivalent conicity is 0.15. Each modal is indicated by a symbol '+', and a larger one represents a larger running speed. The horizontal axis and the vertical axis represent the modal damping ratio (the negative value indicates a stable state) and the damped vibration frequency, respectively. Generally, the hunting modal damping decreases as the running speed increases. When the $\overline{\zeta}$ is greater than 0, hunting instability arises.

The linear stability of the vehicle system is affected by the hunting modal whose frequency is 1–6 Hz. Comparing the speed root locus curves corresponding to the four groups of suspension parameter sets, it can be found that they conform to the classification of suspension parameter sets in the above paragraphs. The modal frequencies corresponding to *Par A* and *Par D* are relatively small, the modal damping ratios of

Table 3. Optimal selection of the suspension parameter sets.

Csy (kN.s/m)	*Kpx* (kN/mm)	*Kpy* (kN/mm)	*Csx* (kN.s/m)	*Kncsx* (kN/mm)	ζ_{low}	ζ_{high}	$std(\zeta_\lambda)$	*Par*
40	58.8	3.41	3750	5.27	−0.34	−0.08	0.12	*A*
10	28.1	4.38	340.2	20.0	−0.09	−0.03	0.02	*B*
40	18.7	3.82	405.4	23.5	−0.08	−0.19	0.07	*C*
40	81.4	3.26	1130	6.07	−0.18	−0.15	0.07	*D*

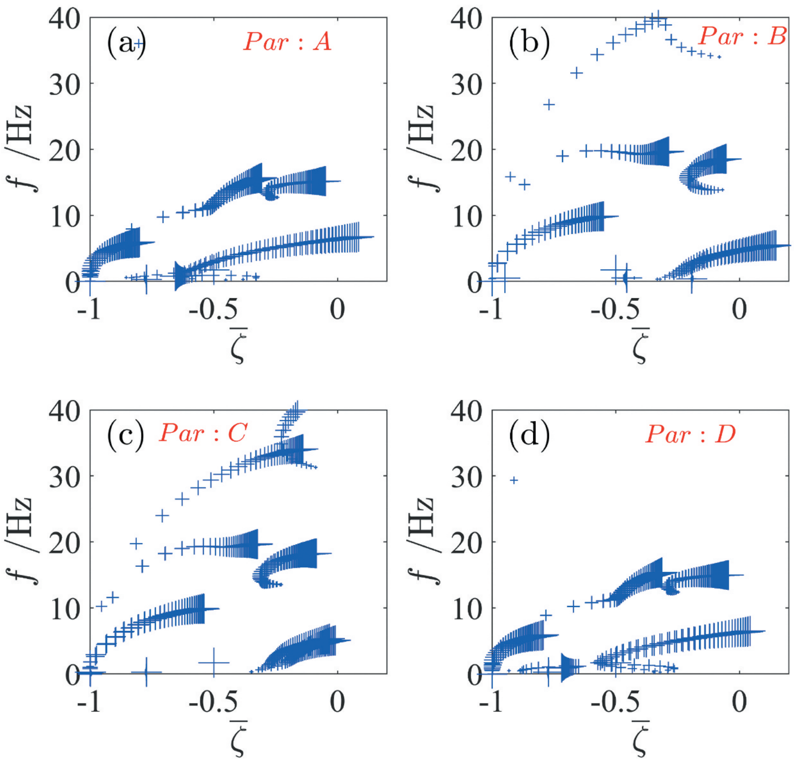

Figure 5. Root loci of the vehicle system with the change of speed.

bogie hunting motion have a large span varying with the running speed, and the vehicle system has a large hunting stability margin at the speeds of 200 km/h and 350 km/h. However, the system stability margins corresponding to *Par B* and *Par C* are relatively poor, but the hunting stability is less sensitive to the variation in speeds, that is, the vehicle system has strong speed robustness, especially for one equipped with the suspension parameters of *Par C*. According to the different characteristics of the root loci of the vehicle system, appropriate suspension parameter sets can be selected for trains at different speed levels.

The root loci of the vehicle system with the change of equivalent conicity are obtained by adopting the suspension parameter sets in Table 3, as depicted in Figure 6. Each root locus curve is composed of 29 sets of characteristic roots in the equivalent conicity range of 0.02–0.6. Each 'o' indicates a corresponding modal, and the larger symbol represents a higher equivalent conicity. The running speed of the vehicle system is 350 km/h. Normally, as the equivalent conicity increases, the hunting modal damping increases first and then decreases. The hunting modal whose frequency varies from 1 to10 Hz dominates the linear stability of the vehicle system.

The root loci of the vehicle system are also consistent with the classification of optimal suspension parameter sets. The root loci of the bogie hunting modals corresponding to *Par B* and *Par C*, which include a smaller *Csx* and a larger *Kncsx*, are similar. When the normal equivalent conicity is located at the turning position of the bogie hunting root

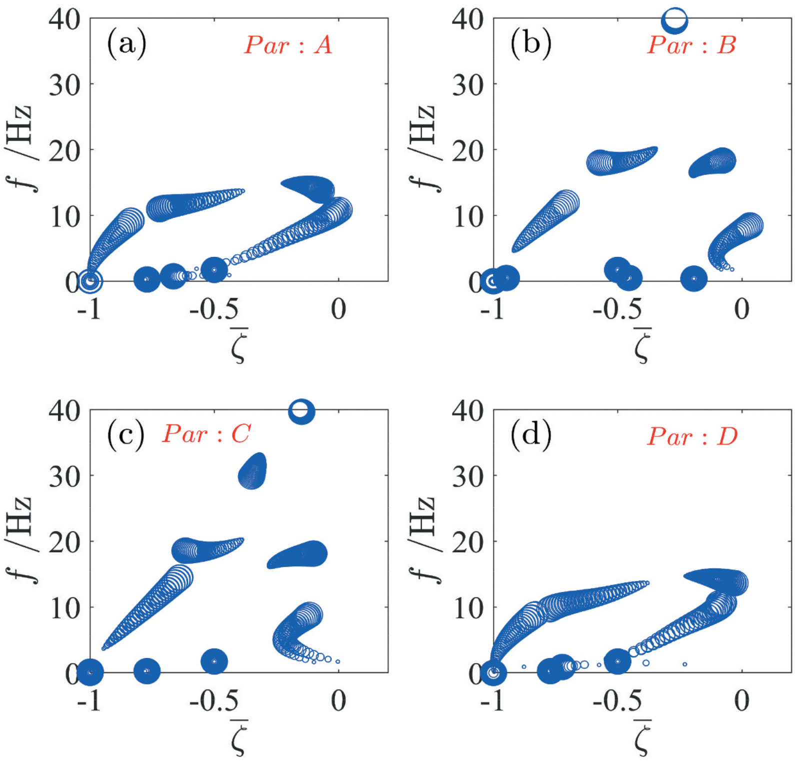

Figure 6. Root loci of the vehicle system with the change of equivalent conicity.

locus, the equivalent conicity robustness index of the vehicle is small, and the hunting stability is insensitive to the variation of wheel–rail contact equivalent conicity. In other words, when the equivalent conicity changes due to the variation in rail cants, wheel profile wear and rail head wear, the stability of the vehicle system changes little. In this way, the vehicle has strong adaptability to the rail line, which is conducive to extending the intervals of track maintenance and wheel reprofiling, thus reducing the costs of operation and maintenance for rail lines and trains. However, it should be noted that the vehicle system is prone to hunting instability due to the insufficient stability margin under the condition of low or high wheel–rail contact conicity. The modal damping of bogie hunting motion corresponding to *Par A* or *Par D* decreases rapidly with the increase of equivalent conicity, indicating poor stability robustness. But the vehicle system has good lateral stability with the normal and low equivalent conicity. These two kinds of characteristics of the root locus all can be found in the practical application, which reflects the two methods for lateral stability design of high-speed trains.

Further analysing the combined effect of running speed and equivalent conicity on the hunting stability of the vehicle, four contour plots of the linear stability index obtained by simultaneously changing the running speed and equivalent conicity are shown in Figure 7. The increment between contour lines is 0.05. When the variation range of the stability index along the longitudinal axis is small, it can be drawn that the change of running speed has a little influence on hunting stability, indicating the strong

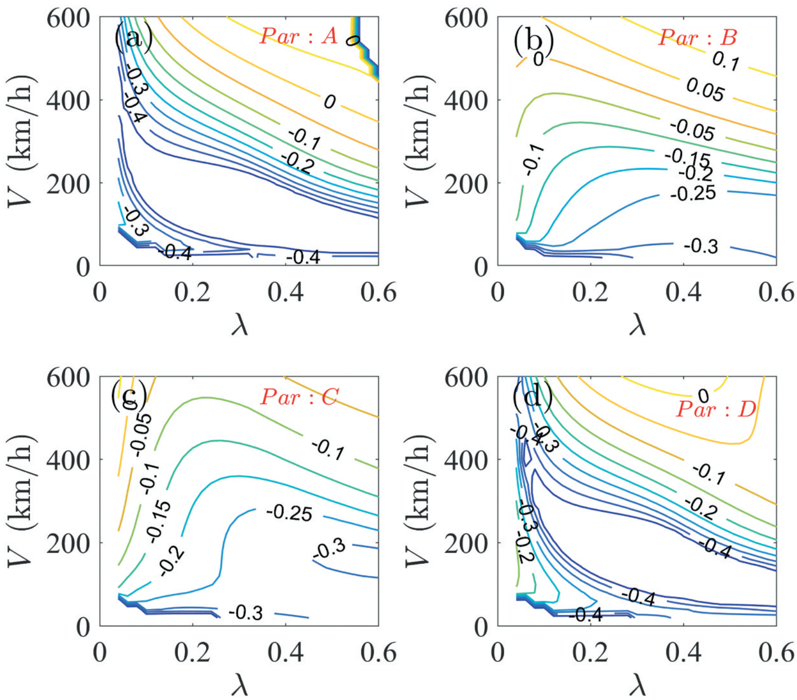

Figure 7. Stability indices varying with equivalent conicity and speed.

speed robustness of hunting stability. As can be observed from the graphs, the effect of running speed on the stability of the vehicle with the low equivalent conicity is smaller than the vehicle with the high equivalent conicity.

The contour plots corresponding to *Par A* and *Par D* have the similar trend, and there are larger stability regions. At a speed of 200 km/h, a large stability margin always can be found varying with the equivalent conicity. And the suspension parameters should avoid being matched with the high equivalent conicity to ensure good hunting stability of the vehicle operating at the speed of 350 km/h. As for *Par B* and *Par C*, the variation of the stability index is gentle but the hunting stability margin is relatively small. The stability index changes little along the horizontal axis, which indicates that the vehicle has strong equivalent conicity robustness. With a low equivalent conicity, the hunting stability of the vehicle system is poor. Therefore, a higher equivalent conicity should be selected to match the suspension parameters to achieve good lateral stability. For the high-speed train operating at the speed of 350 km/h, adopting the suspension parameters of *Par B* is not a good choice for an inadequate stability margin, but it can be applied to the train operating at the speed less than 250 km/h to obtain excellent stability robustness.

Based on the analyses of the root loci and contour plots, two kinds of hunting stability characteristics can be found, and the large stability margin always contradicts hunting stability robustness, which determines the two patterns of suspension parameter design to ensure the hunting stability of the vehicle. That is, suspension parameters can be designed to make the vehicle has a large hunting stability margin but at the expense of stability robustness, or they are selected to improve hunting stability robustness but with the relatively small stability margin.

5. Parameter optimization for motor flexible suspension

The motor suspended flexibly under the bogie frame can realize the mass and inertia decoupling of the motor and frame, which is beneficial to improve the vehicle's critical speed. The stiffness and damping of the motor suspension have a strong influence on the lateral stability of the vehicle; thus, it is necessary to select them reasonably.

Two motors are symmetrically attached to the frame relative to the centre for the power bogie, and the mass of each motor is 850 kg. In this paper, the lateral stiffness and damping of the motor flexible suspension system connected in parallel are optimally designed, the suspension frequency f_{my} and damping coefficient ζ_{my} are used to facilitate the mechanism analysis of the motor suspension system. The f_{my} varies from 0 to 10 Hz, the calculation range of ζ_{my} (positive sign indicates a stable value) is from 0 to 1. Given the above analysis for the high-speed train operating at a speed of 350 km/h, the equivalent conicity is chosen as 0.08 for *Par A* and *Par D*, and 0.25 for *Par B* and *Par C*. Figure 8 shows the hunting stability indices corresponding to the four groups of suspension parameter sets, in which the increment between contour lines is 0.05. The contour plots are consistent with the classification of suspension parameter sets. The optimal f_{my} corresponding to *Par A* and *Par D* is 1 Hz and it is about 3 Hz for *Par B* and *Par C*, which can be explained by the mechanism of dynamic vibration absorber. When the motor suspension frequency is close to the bogie hunting frequency, the lateral vibration of the frame can be suppressed significantly, thus effectively improving the lateral stability of the vehicle system [26]. The difference between the optimal motor suspension frequencies results from the matching equivalent conicity. As shown in Figure 6, higher equivalent conicity normally leads to higher bogie hunting modal

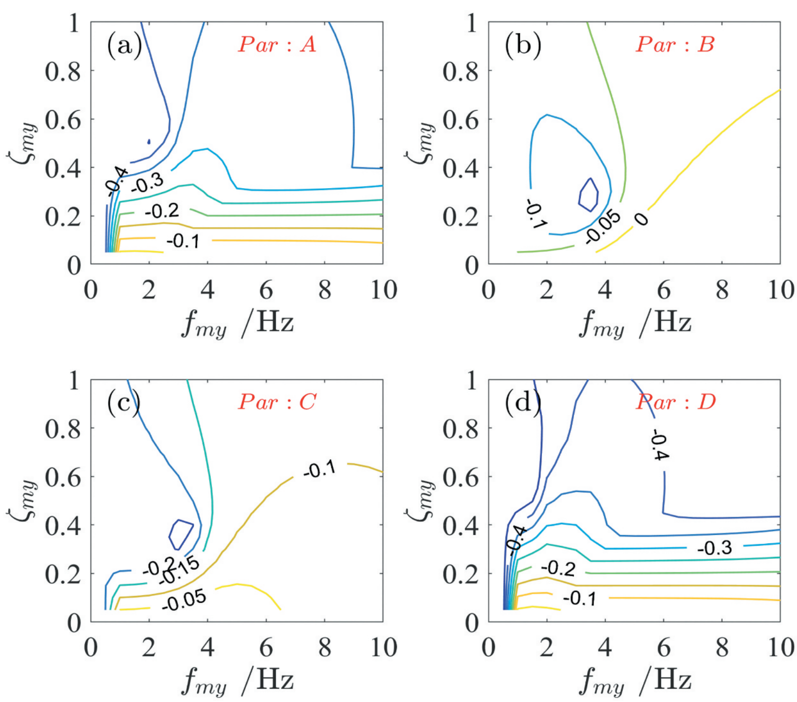

Figure 8. Stability indices with different motor suspension parameters.

frequency, thus a higher f_{my} is required. As for suspension parameter sets *Par A* and *Par D*, the optimal ζ_{my} is 0.5, a large hunting stability margin can be achieved, and the motor suspension parameters can be chosen in a wide range to obtain adequate stability, but the improvement of hunting stability is not obvious compared with the condition without motor flexible suspension. The optimal ζ_{my} corresponding to *Par B* and *Par C* is about 0.3, the hunting stability has been improved remarkably and has reached an adequate margin for engineering application, making it possible to meet the requirements of both satisfactory stability margin and excellent stability robustness.

Selecting appropriate motor suspension parameters can effectively inhibit the lateral vibration of the frame, but the displacement of the motor relative to the frame may be amplified, which is undesired for drive components. Exploring motor active suspension technology is an effective method to solve this problem and has broad research prospects [27,28].

6. Conclusions

(1) Aiming at the hunting stability of high-speed trains, the robust stability indices of low equivalent conicity stability, high equivalent conicity stability and equivalent conicity robustness are defined. The key suspension parameters significantly affecting vehicle hunting stability are optimized by means of the genetic algorithm of NSGA-II. The optimized suspension parameters obtained by this method can meet the requirement of vehicle hunting stability and improve the vehicle's adaptability to different wheel–rail matching in a wide speed range.

(2) The Pareto set of multi-objective optimization based on robust hunting stability reflects the matching characteristics of the optimized suspension parameters. Small secondary lateral damping matches the small damping of yaw damper. Large secondary lateral damping should be matched with the small primary longitudinal stiffness, and the matching damping of yaw damper is either large or small. All these matching laws can be found in engineering applications. The series stiffness of yaw damper affects the stability of the vehicle with the low equivalent conicity significantly, and decreasing the stiffness value is conducive to improving the vehicle stability.

(3) Four groups of optimal suspension parameter sets are selected based on their respective optimal objective performances, they can be divided into two types according to the robust stability characteristics. The first one is the matching of large yaw damping and small series stiffness of yaw damper, and a wheel tread with the low equivalent conicity is required, with which the hunting stability margin of the vehicle is large. The second one is the matching of small yaw damping and large series stiffness of yaw damper, and the high equivalent conicity is needed to ensure hunting stability, with which the vehicle system has good speed robustness and equivalent conicity robustness.

(4) The optimal suspension frequencies of the motor flexible suspension for the two types of parameter sets are about 1 and 3 Hz, respectively. And the optimal damping coefficients of the motor flexible suspension are 0.5 and 0.3, respectively. For the parameter sets achieving a large stability margin, the motor suspension parameters have a wide acceptable range. For the parameter sets achieving strong

stability robustness; however, the parameter optimization of motor flexible suspension can improve the hunting stability of the vehicle significantly, obtaining an adequate stability margin. Therefore, the motor flexible suspension often needs to be used in the engineering application when the second kind of parameter matching sets are adopted.

Disclosure statement

No potential conflict of interest was reported by the authors.

Funding

The material in this paper is based on work supported by grants (51675443, 51735012) from the National Natural Science Foundation of China, National Railway Group Science and Technology Program grant (N2020J026), National Science and Technology Support Program grant (2018YFB1201703), and Traction Power State Key Laboratory grant (No. 2019TPL_Q07, No. 2019TPL_Q08) of the Independent Research and Development Projects.

References

[1] Zhai W, Liu P, Lin J, et al. Experimental investigation on vibration behaviour of a CRH train at speed of 350 km/h. Int J Rail Transp. 2015;3(1):1–16. .
[2] Pearson JT, Goodall RM, Mei TX, et al. Active stability control strategies for a high speed bogie. Control Eng Practice. 2004;12(11):1381–1391.
[3] Allotta B, Pugi L, Colla V, et al. Design and optimization of a semi-active suspension system for railway applications. J Mod Transp. 2011;19(4):223–232. .
[4] Yao Y, Wu G, Sardahi Y, et al. Hunting stability analysis of high-speed train bogie under the frame lateral vibration active control. Veh Syst Dyn. 2018;56(2):297–318. .
[5] Yao Y, Li G, Sardahi Y, et al. Stability enhancement of a high-speed train bogie using active mass inertial actuators. Veh Syst Dyn. 2019;57(3):389–407. .
[6] Zhang X, Wu G, Li G, et al. Actuator optimal placement studies of high-speed power bogie for active hunting stability. Veh Syst Dyn. 2020;58(1):108–122. .
[7] Fu B, Giossi RL, Persson R, et al. Active suspension in railway vehicles: a literature survey. Railway Eng Sci. 2020;28(1):3–35. .
[8] Sun J, Chi M, Wu X. et al. Analysis of the influence of the yaw damper parameters on the vehicle stability. J Vib Meas Diagn [In Chinese]. 2018;38(6):71–76+207.
[9] Chen Z, Zhai W, Lv K. et al. Investigation on influence of the suspension parameters on running stability for suspended monorail vehicle. J Railw Sci Eng [In Chinese]. 2018;15 (10):2647–2653.
[10] Ashtiani IH. Optimization of secondary suspension of three-piece bogie with bevelled friction wedge geometry. Int J Rail Transp. 2017;5(4):213–228.
[11] Pandey M, Bhattacharya B. Effect of bolster suspension parameters of three-piece freight bogie on the lateral frame force. Int J Rail Transp. 2020;8(1):45–65.
[12] He Y, Mcphee J. Multidisciplinary optimization of multibody systems with application to the design of rail vehicles. Multibody Syst Dyn. 2005;14(2):111–135.
[13] Mohebbi M, Rezvani MA. Multi objective optimization of aerodynamic design of high speed railway windbreaks using Lattice Boltzmann Method and wind tunnel test results. Int J Rail Transp. 2018;6(3):183–201.
[14] Ye Y, Qi Y, Shi D, et al. Rotary-scaling fine-tuning (RSFT) method for optimizing railway wheel profiles and its application to a locomotive. Railway Eng Sci. 2020;28(2):160–183. .

[15] Johnsson A, Berbyuk V, Enelund M. Pareto optimisation of railway bogie suspension damping to enhance safety and comfort. Veh Syst Dyn. 2012;50(9):1379–1407.
[16] Bideleh SMM, Berbyuk V, Persson R. Wear/comfort Pareto optimisation of bogie suspension. Veh Syst Dyn. 2016;54(8):1053–1076.
[17] Bideleh SMM. Robustness analysis of bogie suspension components Pareto optimised values. Veh Syst Dyn. 2017;55(8):1189–1205.
[18] Jiang Y, Wu P, Zeng J, et al. Multi-parameter and multi-objective optimisation of articulated monorail vehicle system dynamics using genetic algorithm. Veh Syst Dyn. 2020;58 (1):74–91. .
[19] Yao Y, Li G, Wu G, et al. Suspension parameters optimum of high-speed train bogie for hunting stability robustness. Int J Rail Transp. 2020;8(3):195–214. .
[20] Alonso A, Gimenez JG, Gomez E. Yaw damper modelling and its influence on the railway dynamic stability. Veh Syst Dyn. 2011;49(8):1367–1387.
[21] Sun J, Chi M, Wu X. et al. Hunting motion stability of wheelset based on energy method. J Traff Transp Eng [In Chinese]. 2018;18(2):82–89.
[22] Siinivas N, Deb K. Multiobjective optimization using nondominated sorting in genetic algorithms. Evol Comput. 1994;2(3):221–248.
[23] Yu Y, Zhou C, Zhao L. Optimization of vertical random vibration and damping parameters of high-speed train. 2019;41(9):34–42. J China Railw Soc [In Chinese].
[24] Huan R, Chen L, Sun J. Multi-objective optimal design of active vibration absorber with delayed feedback. J Sound Vib. 2015;339:56–64.
[25] Deb K, Pratap A, Agarwal S, et al. A fast and elitist multi-objective genetic algorithm: NSGA-II. IEEE Trans Evol Comput. 2002;6(2):182–197. .
[26] Yao Y, Zhang H, Luo S. The mechanism of drive system flexible suspension and its application in locomotives. Transport. 2015;30(1):69–79.
[27] Yao Y, Yan Y, Hu Z, et al. The motor active flexible suspension and its dynamic effect on the high-speed train bogie. J Dyn Sys Meas Control. 2017;140(6):064501. .
[28] Yao Y, Zhang X, Liu X. The active control of the lateral movement of a motor suspended under a high-speed locomotive. J Rail Rapid Transit. 2016;230(6):1509–1520.

Appendix

Table A1. The vehicle model parameters.

Item	Value	Unit
Wheelset mass	1639	kg
Yaw inertia of wheelset	822	kg.m^2
Bogie frame mass	2328	kg
Yaw inertia of bogie frame	4080	kg.m^2
Car body mass	38,936	kg
Roll inertia of car body	9.61e5	kg.m^2
Yaw inertia of car body	1.67e6	kg.m^2
Primary vertical stiffness per axle box	0.75	kN/mm
Primary vertical damping coefficient per axle box	10	kN.s/m
Secondary longitudinal stiffness	0.133	kN/mm
Secondary lateral stiffness	0.133	kN/mm
Secondary vertical stiffness	0.2	kN/mm
Secondary vertical damping coefficient	10	kN.s/m
Secondary lateral damping coefficient	10,25,40	kN.s/m
Series stiffness of secondary lateral damping	10	kN/mm
Stiffness of anti-roll torsion bar	4.15	MN.m/rad
Lateral spacing of primary suspension	2000	mm
Length of axle box arm	480	mm
Wheel base	2500	mm
Length between bogie centres	17,375	mm
Distance of contact spot	1493	mm
Lateral spacing of secondary stiffness	1900	mm
Lateral spacing of secondary vertical damping	2646	mm
Lateral spacing of secondary longitudinal damping	2550	mm
Wheel rolling radius	460	mm
Longitudinal creep coefficient	1e7	N
Lateral creep coefficient	1e7	N
Equivalent conicity	0.15	-
Primary longitudinal stiffness	Optimized	kN/mm
Primary lateral stiffness	Optimized	kN/mm
Yaw damper damping coefficient	Optimized	kN.s/m
Series stiffness of yaw damper damping	Optimized	kN/mm